Role of RUNX2 transcription factor in epithelial mesenchymal transition in non-small cell lung cancer: Epigenetic control of the *RUNX2* P1 promoter

Angélica María Herreño[1], Andrea Carolina Ramírez[1] [iD],
Viviana Paola Chaparro[1], María José Fernandez[2], Alejandra Cañas[3],
Carlos Fabian Morantes[4], Olga María Moreno[1], Ricardo Elias Brugés[3],
Juan Andrés Mejía[5], Fernando José Bustos[6], Martín Montecino[6] and
Adriana P Rojas[1] [iD]

Abstract

Lung cancer has a high mortality rate in men and women worldwide. Approximately 15% of diagnosed patients with this type of cancer do not exceed the 5-year survival rate. Unfortunately, diagnosis is established in advanced stages, where other tissues or organs can be affected. In recent years, lineage-specific transcription factors have been associated with a variety of cancers. One such transcription factor possibly regulating cancer is *RUNX2*, the master gene of early and late osteogenesis. In thyroid and prostate cancer, it has been reported that *RUNX2* regulates expression of genes important in tumor cell migration and invasion. In this study, we report on *RUNX2/p57* overexpression in 16 patients with primary non-small cell lung cancer and/or metastatic lung cancer associated with H3K27Ac at P1 gene promoter region. In some patients, H3K4Me3 enrichment was also detected, in addition to WDR5, MLL2, MLL4, and UTX enzyme recruitment, members of the COMPASS-LIKE complex. Moreover, transforming growth factor-β induced *RUNX2/p57* overexpression and specific RUNX2 knockdown supported a role for RUNX2 in epithelial mesenchymal transition, which was demonstrated through loss of function assays in adenocarcinoma A549 lung cancer cell line. Furthermore, RUNX2 increased expression of epithelial mesenchymal transition genes *VIMENTIN, TWIST1*, and *SNAIL1*, which reflected increased migratory capacity in lung adenocarcinoma cells.

Keywords

RUNX2, epithelial mesenchymal transition, lung cancer, epigenetic, histone

[1]Instituto de Genética Humana, Facultad de Medicina, Pontificia Universidad Javeriana, Bogotá, Colombia
[2]Departamento de Ciencias Fisiológicas, Pontificia Universidad Javeriana, Bogotá, Colombia
[3]Departamento de Medicina Interna, Hospital Universitario San Ignacio, Bogotá, Colombia
[4]Facultad de Ciencias Naturales y Matemáticas, Universidad del Rosario, Bogotá, Colombia
[5]Servicio de Radiología e Imágenes Diagnósticas, Hospital Universitario San Ignacio, Bogotá, Colombia

[6]Institute of Biomedical Sciences, Facultad de Medicina y Facultad de Ciencias de la Vida, Universidad Andres Bello, Santiago, Chile

Corresponding author:
Adriana P Rojas, Instituto de Genética Humana, Facultad de Medicina, Pontificia Universidad Javeriana, Carrera 7 No. 40 – 62, Bogotá 110231, Colombia.
Email: rojas-adriana@javeriana.edu.co

Introduction

Lung cancer is the major cause of cancer death in the world, resulting in 1.69 millions of deaths per year.[1,2] Lung cancer is histopathologically classified into two great groups: small cell lung cancer (SCLC) and non-small cell lung cancer (NSCLC), where this later one is the most frequent with 80%–85% patients presenting this type of cancer. In addition, NSCLC is subdivided into three subgroups: large cell carcinoma, squamous cell carcinoma, and the most frequent type adenocarcinoma, with 38% reported cases.[3–5]

In cancer development and progression, normal cells suffer a series of molecular and phenotypic changes, granting them tumor cell phenotype. As described by Hanahan and Weinberg,[6] multistep development of human tumors includes six features: sustained proliferative signaling, evasion of growth suppressors, resistance to cell death, induced angiogenesis, capability of eliciting replicative immortality, and activation of invasion and metastasis.

Epithelial mesenchymal transition (EMT) is an event where cells lose their epithelial properties, while acquiring mesenchymal characteristics.[7–9] During this process, it has been demonstrated that there are strong changes in epithelial and mesenchymal gene expression, regulated by important transcription and signaling factors.[9] In general, EMT is characterized by low *E-CADHERIN* and increased *N-CADHERIN* and *VIMENTIN* expression. For different types of cancer, EMT has been associated with a poor patient outcome and resistance to treatment.[8,10] E-CADHERIN (CDH1) and N-CADHERIN are molecules of the CADHERIN family, fundamental in adherence and tissue maitenance.[10] In addition, several transcription factors (TFs), such as TWIST1 and SNAIL1, have been reported to participate in *E-CADHERIN* suppression, directly binding to their promoter region, thus actively participating in cell migration and invasion.[11–14]

In past years, lineage-specific TFs have been reported to take part of pathophysiological changes, favoring tumor cell proliferation and invasion.[15] RUNX TFs are key regulators of lineage specification. They are associated with major developmental pathways, such as transforming growth factor-β (TGF-β), WNT, Indian hedgehog, NOTCH, receptor tyrosine kinases, and mammalian STE20-like protein kinase (MST)–yes-associated protein 1 (YAP1).[16] RUNX proteins have multiple roles in cancer pathogenesis: in some cancers, they are strong tumor suppressors, while in others, they are oncogenic. Uncontrolled *RUNX* expression is frequently observed in diverse cancer types and has been shown to play major roles in the carcinogenic process.[16]

During early and late embryogenesis, *RUNX2* is essential for osteoblast cell differentiation and bone development.[17] In humans, RUNX2 encodes two isoforms from two alternative promoters, namely RUNX2-type I (also called Cbfα1/p56) and RUNX2-type II (also called Cbfα1/p57).[18] RUNX2/p56 is controlled by the proximal P2 promoter and represents the major RUNX2 isoform in tumor cells.[17] In contrast, RUNX2/p57 is controlled by the distal P1 promoter. There is a differential distribution in type I and II isoforms, not only regarding their spatio-temporal expression, but also with respect to the tissues that express them. In addition, expression can vary depending on species. Observations at tissue level revealed both isoforms exist in bone and lung, whereas RUNX2/p56 is widely expressed in heart, brain, spleen, and skeletal muscles.[18] RUNX2 expression in breast, colon, and thyroid cancer has been demonstrated to be important in tumor cell invasion.[19–21] In prostate cancer, Yuen et al.[22] demonstrated *RUNX2* was correlated with increased prostate-specific antigen (PSA). In lung cancer, Tandon et al.[23] demonstrated *RUNX2* overexpression was associated with bone morphogenetic protein-3B (BMP-3B/GDF10) silencing. However, it is unknown which RUNX2 isoform expression is altered and what is the contribution to EMT in lung cancer.

In this study, we detected increased in *RUNX2/p57* expression in patients with primary and metastatic NSCLC. Interestingly, results demonstrated increases in mRNA expression were greater in patients with primary lung cancer in comparison with patients with metastatic cancer. For all analyzed patients, transcriptional activation of *RUNX2/p57* was associated with enrichment of H3K27Ac at P1 gene promotor region. However, it is important to highlight that in four analyzed patients, additional enrichment of H3K4Me3 occurred simultaneously with enzymes of the COMPASS-LIKE complex: WDR5, MLLl2, MLL4, UTX. On the other hand, silencing experiments allowed to establish RUNX2 TF participated in transcriptional regulation of *E-CADHERIN, VIMENTIN, TWIST1*, and *SNAIL1*, affecting A549 lung adenocarcinoma cell migratory capacity.

Materials and methods

This study included tissue specimens from 16 patients (10 primary lung cancer and 6 secondary lung cancer or metastatic cancer) with histopathologically verified lung masses (Table 1). Patients underwent surgical resection between January and May 2017 at the Hospital Universitario San Ignacio/Bogotá, Colombia. Research was performed under the Colombian Ministry of Health guidelines (No. 008430, 1993) and approved by the Pontificia Universidad Javeriana School of Medicine Ethics Committee. All procedures were carried out after written signed informed consent was obtained from all participants.

Table 1. Clinical characteristics of all cancer patients.

Case	Age	Sex	Pathology Cancer	Pathological diagnosis	Origin	Origin Lung	Origin Other	TNM classification T	N	M	Stage	Comorbidity	One-year survival	Smoker	Treatment
1	66	F	+	Infiltrating adenosquamous carcinoma	Primary	+		4	1	0	IIB	Present	N	N	N
2	77	M	+	Lung adenocarcinoma	Primary	+		3	2A	0	IV	Present	N	Y	Y
3	59	F	+	Pulmonary adenocarcinoma of lepidic pattern	Primary	+		1	0	0	IA	Present	Y	Y	N
4	62	M	+	Lung adenocarcinoma	Primary	+		4	0	1	IV	Absent	N	Y	N
5	44	F	+	Primary adenocarcinoma of the papillary lung	Primary	+		3	2	0	IIIA	Present	N	N	N
6	63	F	+	Poorly differentiated squamous cell	Primary	+		4	3	1	IV	Present	N	Y	N
7	62	M	+	Lung adenocarcinoma	Primary	+		3	3	1	IV	Absent	N	N	Y
8	69	M	+	Poorly differentiated squamous cell carcinoma	Primary	+		4	X	X	IIIA	Present	N	Y	Y
9	60	F	+	Lung adenocarcinoma	Primary	+		3	x	IB	IV	Present	N	Y	Y
10	81	M	+	Lung adenocarcinoma	Primary	+		3	0	0	IIA	Present	Y	Y	Y
11	81	F	+	Mucinous adenocarcinoma	Metastatic		Colon	3	2A	0	IV	Present	Y	N	Y
12	40	F	+	Ductal adenocarcinoma of the mammary gland	Metastatic		Breast	3	1	0	IIIA	Present	N	Y	Y
13	66	F	+	Endometrial adenocarcinoma	Metastatic		Endometrial	2	x	0	II	Present	Y	Y	N
14	80	F	+	Kidney adenocarcinoma	Metastatic		Kidney				IV	Present	N	N	N
15	69	F	+	Solitary fibrous tumor	Metastatic		Pleural	4	2	1	IV	Present	Y	N	Y
16	67	M	+	Poorly differentiated carcinoma	Metastatic		Pancreatobiliary	3	2	1	IV	Absent	N	Y	Y

M: male; F: female; N: no; Y: yes.

Cell culture

Primary cell culture was established from biopsies following our protocol from previous research.[24] From these samples, gene expression and chromatin immunoprecipitation (ChIP) analyses were performed.

Human lung adenocarcinoma cell line A549 (ATCC®; Manassas, VA) was cultured in Dulbecco's Modified Eagle Medium supplemented with 10% fetal bovine serum (FBS) and 5% antibiotics (ampicillin and streptomycin) and incubated at 37°C in humidified 5% CO_2 atmosphere. Cells were grown to 80% confluence to perform silencing and invasion assays. To induce the EMT process, A549 cells were treated with TGF-β1 (10 ng/mL, Abcam 50036) according to Zhang et al.[25]

Lentivirus production and infection of A549 cells

HEK293FT cells (Life Technologies) were grown in 60 mm culture plates to reach 80% to 90% confluence. To transfect cells, Lipofectamine 2000 (Life Technologies) was used with pCMV-VSVg, pCMVdR8.91, and pLKO.1-shRNA plasmids following manufacturer's instructions at a ratio of 1:2:3, respectively, with maximum total DNA of 10 μg per plate. pLKO.1 EV (sh-Ctrl) was used as control. Plasmids were donated by Dr Martín Montecino, Universidad Andrés Bello, Santiago, Chile. After 16–18 h, culture medium was replaced, and cells were maintained at 32°C for 48 h. Supernatants containing pseudo-typed particles were collected and filtered through a polyvinylidene fluoride filter (0.45 μm pore size). Supernatant aliquots were immediately stored at 80°C.[17] A549 cells were plated in 6-well culture plates and infected for 48 or 72 h with shRUNX2 or pLKO.1 EV (empty vector) with 5.779×10^9 copies/mL viral particles and 0.005 mg polybrene.

Nuclear extracts and protein expression analyses

Nuclear extracts were prepared as previously reported.[24] Total protein was quantified by the Bradford assay using bovine serum albumin as standard. For Western blot assays, 15 μg total protein was separated by sodium dodecyl sulfate-polyacrylamide gel electrophoresis transferred to nitrocellulose membranes and immunoblotted. Primary antibodies used were RUNX2 (NBP2-24755SS; Novus Biologicals) and TFIIB C-18 (sc-225; Santa Cruz Biotechnology) as loading control. Immunoblots were visualized by enhanced chemiluminescence system (PerkinElmer Life Sciences). Densitometry was performed on scanned immunoblot images using ImageJ gel analysis tool.[26]

Reverse transcriptase and quantitative real-time polymerase chain reaction

Total RNA was extracted with TRIzol (Life Technologies) according to manufacturer's protocol. An equal amount of each sample (2 μg) was used for reverse transcription. Quantitative real-time polymerase chain reaction (qRT-PCR) was performed using SYBR Green I Master real-time PCR kit (Roche). Data are presented as relative mRNA levels of the gene of interest normalized to GAPDH mRNA levels.

ChIP

To identify regulatory components mediating epigenetic changes related with *RUNX2* transcriptional control during lung cancer progression, ChIP assays were performed in primary cell culture. To this end, cross-linked chromatin samples were employed as described in Rojas et al.[27]

Re-ChIP assays were performed as previously described.[28] Briefly, immunoprecipitated complexes obtained by ChIP were eluted by incubation for 30 min at 37°C in 25 μL of 10 mM dithiothreitol. After centrifugation, supernatant was diluted 20 times with sonication buffer and subjected to ChIP procedure with the second antibody.

Invasion assay

A549 cells infected with shRUNX2 or shCtr were cultured separately until reaching 80% confluence. Cells were then washed three times with phosphate-buffered saline (PBS) and cultured in serum-free media overnight before being subjected to an in vitro extracellular matrix (ECM) protein invasion assay. Invasion assay was conducted using BioCoat Matrigel Invasion Chambers with 8 μm pores (BD Biosciences, Bedford, MA) according to manufacturer's instructions. Briefly, 70,000 cells were resuspended in fresh serum-free media and seeded into the upper chamber of a 24-well transwell plate, while the lower chamber contained fresh culture media with 5% FBS with or without 10 ng/mL TGF-β1. Cells were allowed to invade for 48 h (37°C, 5% CO_2 humidified atmosphere). Chambers were then washed with PBS. Those cells that did not invade through the membrane were removed. Cells that invaded to the lower surface of the membrane were fixed with cold methanol, stained with 0.2% crystal violet, and examined. Cells on each membrane were counted in not less than five fields under a light microscope.

Statistical analyses

To compare significant changes with respect to control (noncancerous tissue (NCT)) for ChIP assays, one-way analysis of variance analysis followed by Dunnett's post hoc test was performed to determine differences. To establish gene expression differences, unpaired Student's *t* test was carried out. In all figures, error bars represent the standard error of the mean (*p < 0.05, **p < 0.01, ***p < 0.001).

Exploratory analyses were performed to determine whether *RUNX2/p57* expression levels were associated with cancer stage, 1-year survival, smoking history, and patient age. Using the median value distribution of *RUNX2/p57* expression levels, participants were grouped into high RUNX2/p57 and low RUNX2/p57 levels; clinical parameters were compared between groups. To establish statistically significant differences between groups, a Student's *t*-paired test was used. Data bivariate normality distribution was then determined, and according to the type of variables, a polychoric correlation, polyserial correlation, or Pearson correlation between variables was performed. The null hypothesis in all cases was rejected with a level of significance of $p < 0.03$. Statistical analyses were carried out employing R statistical software®.

Results

RUNX2/p57 overexpression in tissues of patients with primary lung cancer and secondary cancer with lung metastasis

Real-time qRT-PCR was performed to quantify *RUNX2/p56* and *RUNX2/p57* isoform expression in cancer tissues obtained from 16 cancer patients, 10 with primary lung cancer (patients 1–10) and 6 with secondary cancer with lung metastasis (patients 11–16). We used two samples obtained from non-tumor lung tissue (NCT) as controls. For all samples, *GAPDH* and *β-actin* were used as internal controls to normalize differences in total RNA levels for each sample. Results revealed that 87% (14 out of 16 patients) of tumor tissues had higher *RUNX2/p57* expression levels in comparison with non-tumor tissue (Figure 1 and Supplemental Figure 1). Similarly, expression of *RUNX2/p56* in tumor tissue showed a significant increase in 3 patients. However, it is important to note that overexpression levels were below those detected for *RUNX22/p57* isoform (Figure 1(a) and (b); Supplemental Figure 1(A) and (B)). Figure 1(c) and (d) illustrates protein expression levels by Western blot for seven patients and a non-tumor sample. Results revealed *RUNX2/p57* isoform expression levels were greater in comparison with *RUNX2/p56*. Figure 1(e) depicts percentage increase in RUNX2/p57 in comparison with RUNX2/p56 isoform.
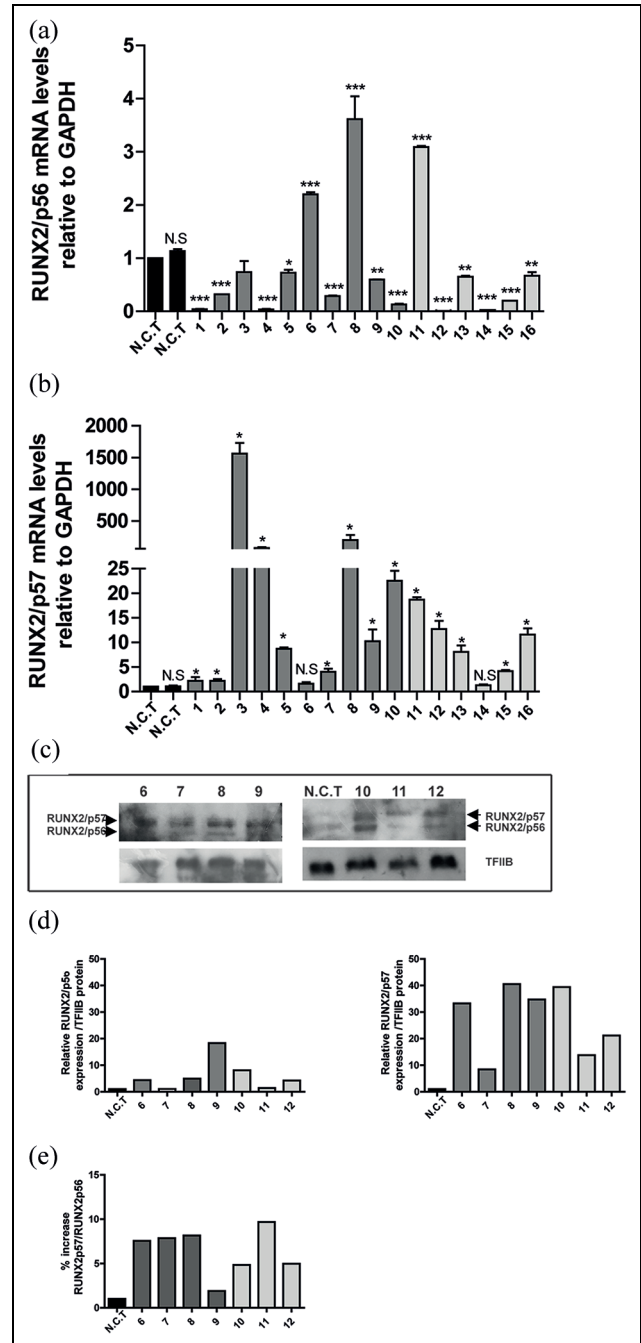

Figure 1. *RUNX2/p57* overexpression in tissues of patients with primary lung cancer and secondary cancer with lung metastasis. *RUNX2/p56* (a) and *RUNX2/p57* (b) relative mRNA expression in lung cancer tissues of patients with primary lung tumor (patients 1–10) and secondary tumors (patients 11–16) compared with noncancerous tissue (NCT). mRNA levels were quantified by qRT-PCR and normalized to GAPDH mRNA. Statistical analyses were performed with respect to NCT. *p < 0.05; **p < 0.01; ***p < 0.001. (c) RUNX2/p56 and RUNX2/p57 protein isoform expression. TFIIB protein levels were used as loading control. RUNX2/p56 and RUNX2/p56 Western blot densitometry was performed using ImageJ. (d) RUNX2-p57/RUNX2-p56 protein percentage increase. (e) Percentage increase in RUNX2/p57 in relation to RUNX2/p56.

Correlation between clinical parameters and expression levels of RUNX2/p57

Table 1 describes study subjects with their clinical characteristics. Data on cancer stage, smoking history, and age were collected at the time of enrolment and after 1 year of patient survival. Using *RUNX2/p57* expression level median value distribution, which was 9.47, participants were grouped in high and low *RUNX2/p57* levels and clinical parameters for comparison between groups. No significant differences were observed for comparisons between participant age, smoking history, and cancer stage and 1-year survival.

Participants were grouped based on cancer origin, with 10 (n = 10) participants with primary lung cancer and 6 (n = 6) participants with metastatic lung tumors. Using *RUNX2/p57* expression median value distribution for each group, participants were grouped into high *RUNX2/p57* and low *RUNX2/p57* levels and clinical parameters were compared between groups. For the lung cancer metastatic group, no differences were observed for comparisons between participant age, smoking history, and cancer stage and 1-year survival.

For the primary lung cancer group, no differences were observed in comparisons between participant age, smoking history, cancer stage, and 1-year survival. Interestingly, a significant difference was observed between high and low *RUNX2/p57* levels for participants with cancer stages II and IV under 16.4 *RUNX2/p57* expression level median value distribution and participants with stage III above *RUNX2/p57* expression level median value distribution. Due to the number of participants, Student's *t*-paired test statistical analysis between groups could not be performed. However, correlations between *RUNX2/p57* expression levels and age, smoking history, and cancer stage and 1-year survival and primary lung cancer were performed. No correlations between age, smoking history, and 1-year survival and *RUNX2/p57* levels were observed. A strong tendency associated with high *RUNX2/p57* expression in stage III was noted (Figure 2). Considering the very small sample size, we believe these findings should be analyzed with caution.

RUNX2/p57 expression in lung tumor cells involves changes in epigenetic histone marks

Transcription of *RUNX2/p57* gene, a master regulator of osteoblast differentiation, is controlled by the P1 promoter sequence, specifically the 500-pb region most proximal to transcription initiation site, which suffers chromatin remodeling in mouse osteoblastic cells during *RUNX2* expression.[27] This promoter region is highly conserved and has been shown to include regulatory elements that are functional within human, rat, and mouse osteoblastic cells.[27] To shed light on the cellular process
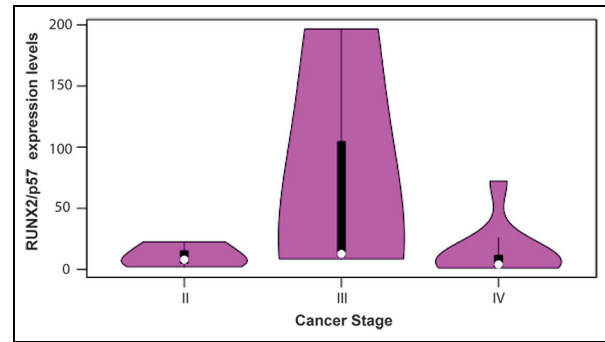

Figure 2. Correlation between expression of RUNX2 and lung cancer stage. There was a strong increased RUNX2 expression tendency in participants at clinical stage III and low RUNX2 expression in participants at clinical stages II and IV. Black boxes represent 50% of data around the median (white circle). Purple areas show data value frequency around the median.

controlling *RUNX2/p57* expression in human lung cancer, contribution of epigenetic mechanisms was assessed. Tumor cells exhibited at the P1 promoter post-translational modifications at histone H3. Thus, enrichment at H3K27Ac was observed with H3K27Me3 reduced levels at the R*UNX2* P1 promoter site (Figure 3(b) and (c)). Surprisingly, we found enrichment of H3K4Me3 in patients 8,9,12, and 13 (patients 8, 9, 12, and 13) (Figure 3(a)). Hence, this epigenetic mark corresponds to the activacion of the P1 promoter during tumor progression.

RUNX2 P1 promoter was recognized by epigenetic regulators during lung tumor progression

In order to identify regulatory components mediating epigenetic changes related with *RUNX2/p57* transcriptional control during lung cancer progression, ChIP analyses were performed. WDR5, MLL2, MLL4, and UTX exhibited a significantly higher enrichment at the proximal *RUNX2* P1 promoter sequence for patients 8, 9, 12, and 13 (Figure 4(a)–(d), respectively).

We have recently shown that during osteoblast commitment, a MLL/COMPASS-LIKE complex plays a relevant role during *RUNX2* transcription.[17] Next, it was determined whether additional subunits (in addition to UTX) of these H3K4 methyltransferase complexes were bound to the *RUNX2* P1 promoter (Figure 4(e)). It was found that MLL2 and MLL4 were enriched at this *RUNX2* P1 promoter sequence (Figure 4(e)).

Increase in RUNX2/p57 expression in A549 cell line tumor progression

To determine whether cells initiated an EMT process, first EMT key markers *E-CADHERIN, N-CADHERIN*, and *VIMENTIN* were quantified in cells
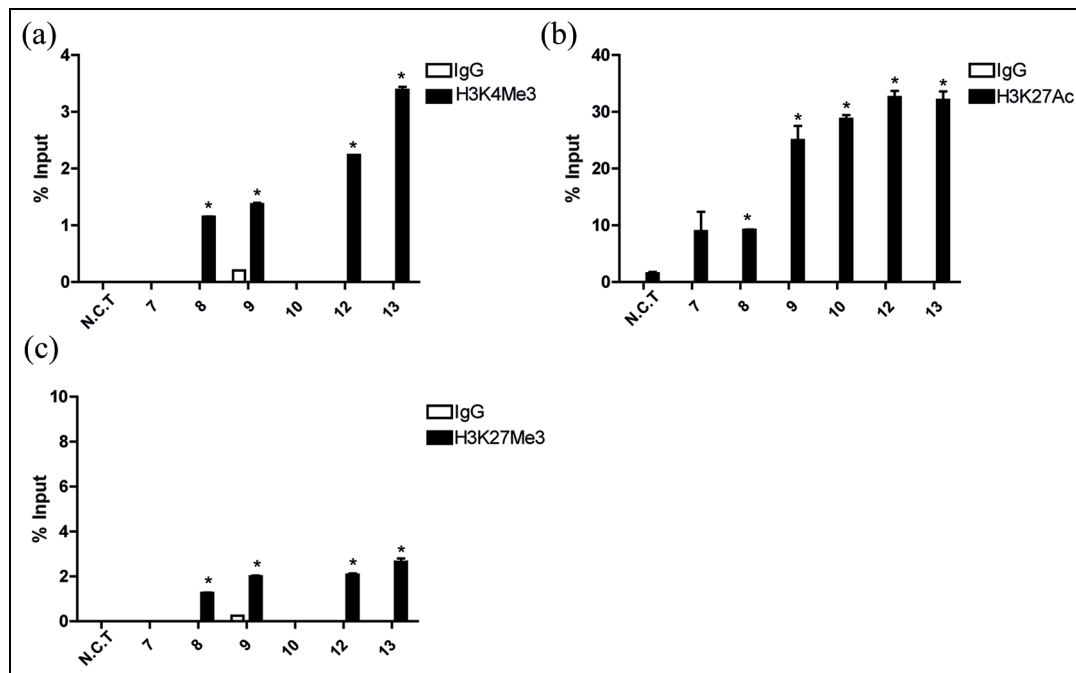
Figure 3. RUNX2 epigenetic transcriptional control. Histone post-translational modifications at *RUNX2* P1 promoter region in lung cancer cells and secondary cancer cells with lung metastasis. Primary lung cancer cells of four patients (patients 7, 8, 9, and 10) and secondary cancer cells (patients 12 and 13) were used to perform ChIP assays. Antibodies against (a) H3K4Me3, (b) H3K27Ac, and (c) H3K27Me3 were used. Results are expressed as % input $\pm$ SEM using normal IgG as specificity control. Statistical analyses were performed with respect to NCT cells.
*p < 0.05.

treated with TGF-β1 (Figure 5(a)–(c); Supplemental Figure 2). Initiation of EMT after stimulation, was observed based on low *E-CADHERIN* epithelial marker expression was detected. In addition, overexpression of *N-CADHERIN* and mesenchymal marker *VIMENTIN* were observed. To assess *RUNX2/p56* and *RUNX2/p57* expression during EMT, mRNA and protein levels were quantified. Results revealed an increased in *RUNX2/p57* expression and protein levels after cells were treated with TGF-β1 (Figure 5(d)–(f); Supplemental Figure 2). Moreover, RUNX2/p56 expression in TGF-β1 treated and untreated cells remained constant (Figure 5(d)–(f); Supplemental Figure 2).

Absence of RUNX2 was associated with decreased EMT markers and TWIST1 and SNAIL1

To determine the role of *RUNX2* in EMT process, we knocked down *RUNX2* using shRNA in TGF-β1 stimulated or unstimulated cells. As shown in Figure 6(a) and (b), utilized shRUNX2 affected both mRNA expression isoforms and proteins (RUNX2/p56 and RUNX2/p57). Expression of *E-CADHERIN, N-CADHERIN, VIMENTIN, TWIST1*, and *SNAIL1* was quantified by qRT-PCR (Figure 6(c)–(g); Supplemental Figure 3). Likewise, for this analysis,

EMT was evaluated in sh-Ctrl (control) treated cells and stimulated or unstimulated with TGF-β1 with the previously mentioned markers (Figure 6(c)–(g)). A decrease in *E-CADHERIN* after *shRUNX2* treatment in TGF-β1 unstimulated cells was detected (Figure 6(c)). Moreover, a decrease in *VIMENTIN* expression was also observed in TGF-β1 treated and untreated cells (Figure 6(e)). In contrast, when *RUNX2* was silenced, *N-CADHERIN* did not show any variation (Figure 6(d)). In addition, cells infected with *shRUNX2* evidenced significant changes in *TWIST1* and *SNAIL1* gene expression (Figure 6(f) and (g); Supplemental Figure 3).

Absence of RUNX2 affect A549 lung adenocarcinoma invasion capacity

To evaluate *RUNX2* A549 lung adenocarcinoma cell capacity to invade, a transwell system was employed (Figure 7). Our results show that shRUNX2 completely inhibited TGF-β-induced invasion, suggesting RUNX2 may be responsible for increased invasion. Quantification of the assay is illustrated in Figure 7. For statistical analysis, control cells were transduced with sh-Ctrl and treated (+) or untreated (–) with TGF-β1.
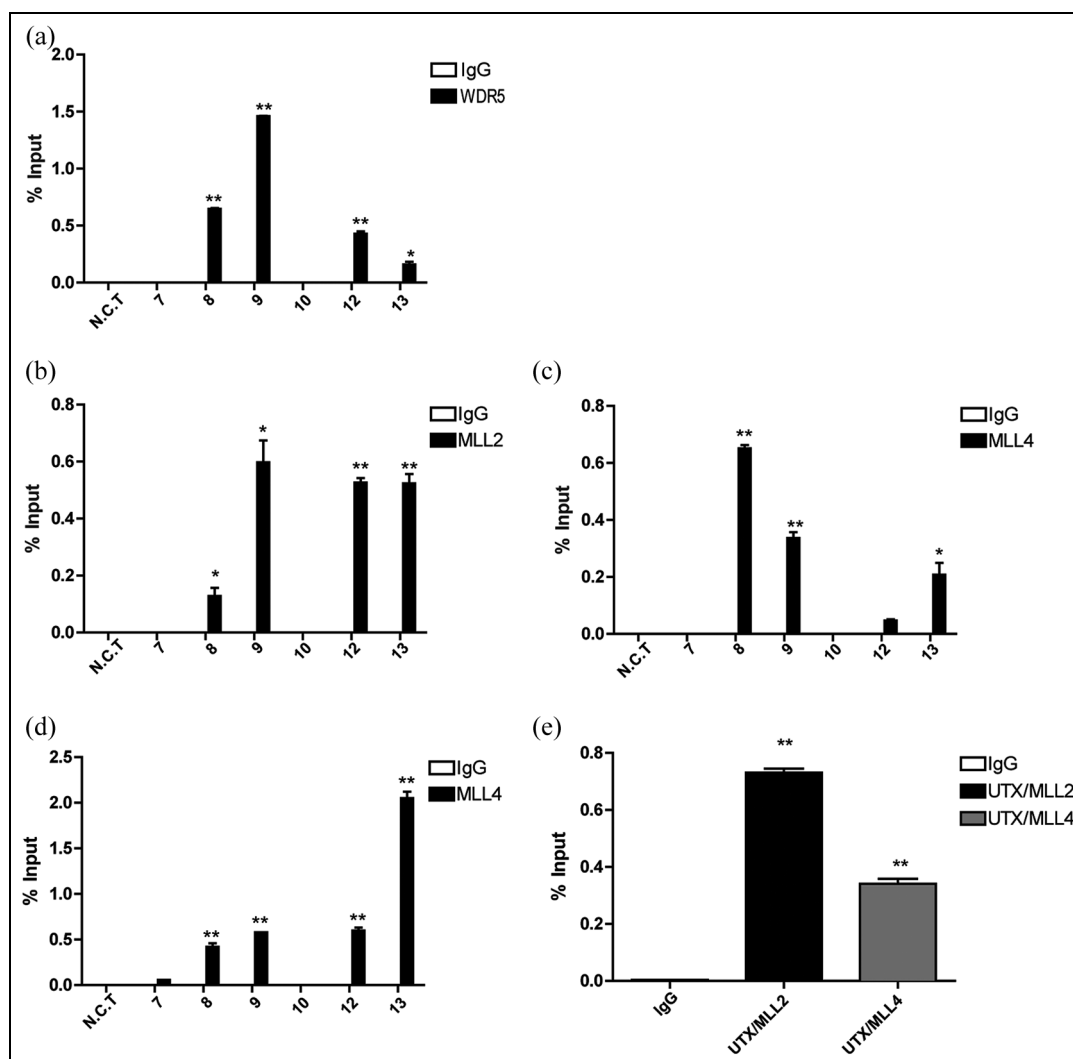
Figure 4. *RUNX2* P1 promoter was recognized by chromatin-modifying enzymes in lung cancer cells and secondary cancer cells with lung metastasis. Primary lung cancer cells of four patients (patients 7, 8, 9, and 10) and secondary cancer cells (patients 12 and 13) were used to perform ChIP assays. Antibodies against chromatin-modifying proteins (a) WDR5, (b) MLL2, (c) MLL4, and (d) UTX were used. Results and statistical analyses are shown as described in previous figure legend. Normal IgG was used as specificity control. $*p < 0.05$; $**p < 0.01$; $***p < 0.001$. (e) Re-ChIP assay was performed using chromatin extracted from the tumor of patient 9. This assay demonstrated *RUNX2* P1 promoter co-occupancy by MLL2, MLL4, and UTX. The first ChIP assay was performed with antibody against UTX, and the second ChIP (Re-ChIP) was carried out with antibodies against MLL2 and MLL4. Controls for the Re-ChIP assay were performed with anti-rabbit and anti-mouse IgG (IgG/IgG).

Discussion

In general, cell identity is regulated by TFs that recognize specific sequences in the genome, and thus regulate gene expression.[29,30] Almost 50% of the TFs encoded in the genome are expressed in any cell type; however, a smaller number of master TFs are sufficient to establish control of gene expression programs, also known as lineage regulators that define cell identity.[29,30] In recent years, these master TFs have been described to participate in neoplastic processes. Activation of a master TF, normally expressed early in a specific lineage, can alter core regulatory circuitry and activate additional genes that are regularly expressed in more embryonic states.[29,30]

It has been described RUNX2, an osteogenic master TF, is engaged in tumor progress, through direct or indirect regulation of genes favoring migration and invasion capacity in different types of cancer.[19,23] In the present study, significantly higher *RUNX2/p57* expression was demonstrated in samples of primary or metastatic lung cancer compared with samples from nontumor tissue. Our results demonstrated mRNA did not precisely correlate with protein levels. Regarding the above mentioned, it has been demonstrated that transcription and translation are far from having a linear
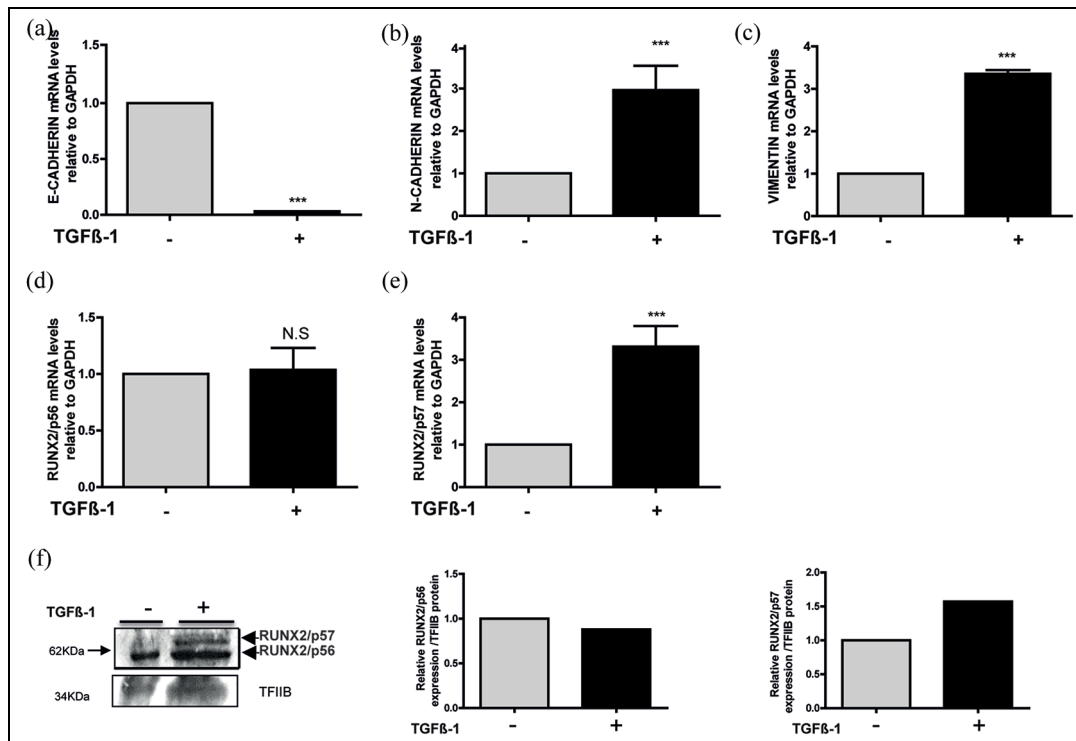
Figure 5. Overexpression of *RUNX2* in A549 cell line induced with TGF-β1 to promote EMT process. Human lung adenocarcinoma A549 cells were pre-cultured with or without 10 ng/mL TGF-β1 for 48 h. (a)–(c) *E-CADHERIN, N-CADHERIN*, and *VIMENTIN* mRNA levels in A549 cells. (d)–(f) *RUNX2/p56* and *RUNX2/p57* mRNA and protein levels in A549 cells with or without TGF-β1 treatment. Statistical analyses were performed with respect to A549 cells without TGF-β1.
*p < 0.05; **p < 0.01; ***p < 0.001.

and simple relationship. Different mechanisms involving *cis*-acting and *trans*-acting mechanisms generate a large repertoire of posibilities, capable of enhancing or repressing protein synthesis from mRNA molecules. Different events may uncouple transcription and translation continuously or under certain conditions.[31] In 2013, Li et al.[20] reported *RUNX2* overexpression in patients with NSCLC lung cancer. However, their work did not analyze *RUNX2/p56* and *RUNX2/p57* isoforms. For other types of cancer, such as breast, prostate and thyroid RUNX2/p56 overexpression has been reported.[20] Specifically, in studies using thyroid and breast cancer cell lines, overexpression has been associated with the presence of H3K27Ac and H3K4Me3 activator marks at the P2 promoter.[17]

In the present study, correlation analyses between clinical parameters and *RUNX2/p57* expression levels allowed to establish an association between *RUNX2/p57* expression level and tumor stage. A strong tendency was established between *RUNX2/p57* high expression levels and stage III. Stage II lung cancer is capable of spreading from the lungs to the lymph nodes or to nearby structures and organs, such as the heart, trachea, and esophagus. In contrast, in stage III, lung cancer has already metastasized to other areas of the

body,[32] suggesting RUNX2 could be involved during the first steps of invasion, when cancer spreads to the lymph nodes and nearby organs. However, considereing the reduced number of patient samples, we believe that that these findings should be analyzed with caution.

In addition, to determine whether *RUNX2/p57* overexpression was related with gene's epigenetic chromatin modifications in associated histones, ChIP assay was carried out. *RUNX2/p57* expression was related with H3K27Ac active enhancer mark enrichment at P1 promoter. Interestingly, 66.6% of analyzed patients by ChIP assay also had a H3K4Me3 active mark enrichment at the promoter region. This enrichment occurred simultaneously with enzyme recruitment of the COMPASS-LIKE complex (WDR5, MLL2, MLL4, and UTX) to the promoter region. Co-presence of UTX, MLL2, and MLL4 complex was additionally confirmed by re-ChIP.

Results are in agreement with those reported by Rojas et al.[27,28] in 2015, where it was demonstrated in mouse mesenchymal cells *RUNX2/p57* transcriptional regulation was determined by existence of a specific pattern of covalent modifications in histone residues. Therefore, during osteoblast differentiation, when the
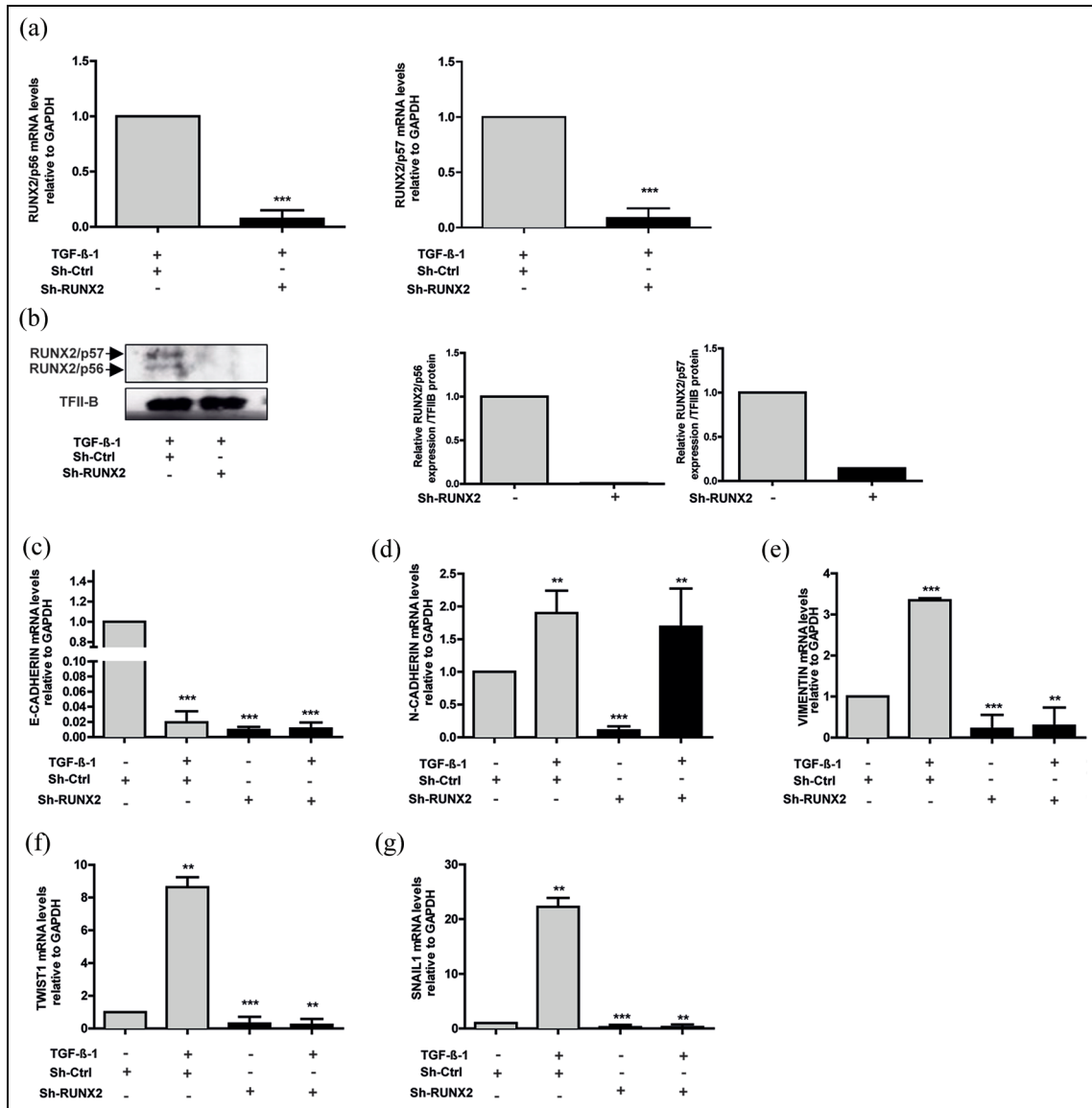
Figure 6. Knockdown of *RUNX2* affects EMT marker expression. A549 cells were stimulated with or without TGF-β1 as described in Figure 4. A549 cells were infected with lentiviral particles coding for shRNAs against *RUNX2*. Effective down-regulation was confirmed by qRT-PCR (a) and Western blot (b) analyses 72 h post infection. TFIIB protein levels were used as loading control (c). *E-CADHERIN*, (d) *N-CADHERIN*, (e) *VIMENTIN*, (f) *TWIST1*, and (g) *SNAIL1* mRNA levels were quantified by qRT-PCR 72 h after infection. Statistical analyses were performed with respect to cells infected with virus generated with the pLKO.1 empty vector (sh-Ctrl.). $*p < 0.05$; $**p < 0.01$; $***p < 0.001$.

gene was transcriptionally active, enrichment of H3K27Ac and H3K4Me3 occurred in parallel with the COMPASS-LIKE complex (WDR5, MLL, UTX) recruitment. In contrast, when cells differentiated into myoblast lineage, enrichment levels of H3K27Ac and H3K4Me3 active marks were significantly decreased, with concomitant increase in repressor mark, such as H3K27Me3, among others.[27,28]

Participation of COMPASS-SET1 and COMPASS-LIKE complexes in cancer has been widely demonstrated. Mixed lineage leukemia (MLL) gene was first discovered as an oncogenic fusion resulting from seemingly random translocations in patients with hematological malignancies.[33] COMPASS complex is capable of catalyzing mono-, di-, and trimethylation on histone H3K4.

In mammals, COMPASS complex is grouped into three categories: COMPASS-Set, Mll1/Mll2 COMPASS (orthologs of Trx in Drosophila), and Mll3/Mll4 COMPASS (orthologs of Trr in Drosophila).[33] To ensure proper transcriptional modulation, a growing body of evidence points to a model,
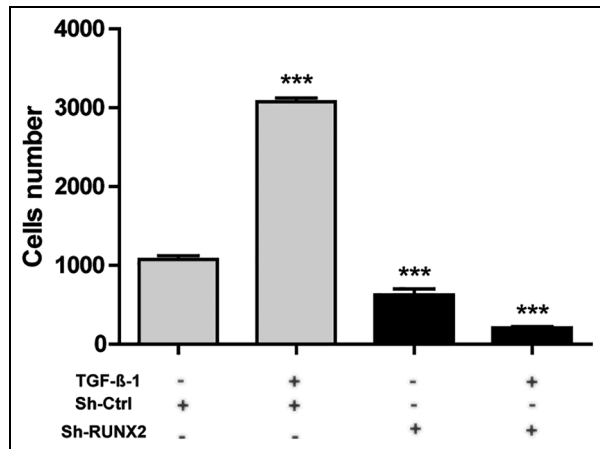
Figure 7. Effect of *RUNX2* knockdown on transwell migration and invasion assay. (a) A549 cells were stimulated with or without 10 ng/mL TGF-β1 and infected with lentiviral particles coding shRNAs against *RUNX2*. Cells penetrating the membrane were fixed and stained after 48 h as described in experimental procedures. Migrating cells were counted after additional incubation with 10 ng/mL TGF-β1 for 48 h.
Data are shown as mean ± SD, ***p < 0.001.

where H3K4 methylation is divided among COMPASS family members.[28] In this way, it has been demonstrated that Mll1/Mll2 is necessary to maintain H3K4 trimethylation levels, whereas Mll3/Mll4 is responsible for H3K4 monomethylation enrichment.[28] These findings would explain presence of Mll2 and Mll4 at the P1 promoter region of *RUNX2* gene in samples from patients with primary and metastatic lung cancer.

Parallel to RUNX's role in EMT during development, in different tissues, these proteins have been implicated in aberrant cancer EMT activation. The best characterized of these phenomena is RUNX2 involvement in breast and prostate cancer metastases.[34] In prostate cancer, it has been demonstrated that RUNX2 positively regulates EMT through direct regulation of *SMAD3, SNAIL2,* and *SOX9* genes. In thyroid cancer, it has also been reported an association between RUNX2 and aberrant EMT through regulation of target genes, such as *SNAIL2, VEGF, TWIST1,* and *MMP2.*[34]

To determine *RUNX2* role in EMT process in lung cancer, *RUNX2* loss of function by shRNA in lung adenocarcinoma A549 cell line was performed. This cell line is widely used to simulate in vitro EMT process under TGF-β1 stimulus, where cells acquire mesenchymal phenotype and their migration capacity is increased.[25] It is important to acknowledge cells infected with shRUNX2 demonstrated decreased expression in both of *RUNX2* isoforms (RUNX2/p56 and RUNX2/p57). Our findings demonstrated EMT

did not occur in cells infected with *shRUNX2*, as shown by low invasion capacity in transwell assay and decreased expression of *VIMENTIN, TWIST1,* and *SNAIL1.* On the other hand, incubation of cells with TGF-β repressed the expression of *E-CADHERIN* in the presence or absence of *RUNX2.*

An important EMT hallmark is loss of cell-to-cell adhesion molecule expression. E-cadherin is a central component of cell–cell adhesion junctions and is required for formation of epithelial tissues in the embryo and to maintain epithelial homeostasis in the adult.[35] Loss of E-cadherin expression is consistently observed at EMT sites during development and cancer. This loss has been found to increase tumor cell invasiveness in vitro and contributes to the transition of adenoma to carcinoma in animal models.[35] Several important proteins during development that induce EMT have been shown to act as E-cadherin repressors or activators. For example, Slug (also known as SNAI2), a member of the Snail family of transcriptional repressors, is capable of repressing E-cadherin expression and thereby triggering EMT,[35] suggesting that it may act as an invasion inducer. It has been acknowledged that both SNAIL and its family member SLUG are capable of repressing E-cadherin in epithelial cells via E-box elements in the proximal E-CADHERIN promoter.[35] Functional assays in the present study demonstrated that TGF-β repressed *E-CADHERIN* in the presence or absence of RUNX2. Hence, it is possible that *E-CADHERIN* may be under the control of other factors. Nonetheless, additional analyses are required to confirm this finding. At present, it is known that this gene is regulated by various TFs. Recently, Li et al.[36] demonstrated RUNX2 TF binds directly to *E-CADHERIN* promoter and positively regulates its activation during epithelial differentiation of adipose-derived stem cells in mammals. *N-CADHERIN* expression increased under TGF-β stimulation and decreased with shRUNX2; however, when TGF-β was added in cells expressing shRUNX2, expression was still increased. This result suggests possibly under TGF-β stimulation, other TFs could have regulated promoter activation.

In addition, we demonstrated an effect on *TWIST1* and *SNAIL1* gene expression, which participate in tumor cell migration, suggesting *RUNX2* exerts a positive regulatory effect on both genes. Moreover, *RUNX2* expression is essential in *TWIST1* and *SNAIL1* activation. Regulation of these genes by RUNX2 has been reported in thyroid tumor cells and lung adenocarcinoma in very advanced cancer stages.[21,23,37] Furthermore, RUNX2 capacity to bind to *TWIST* promoter in neuroblastoma tumor cells has been described.[38]

Our results also demonstrate RUNX2 participated in *VIMENTIN* expression, a mesenchymal marker, since *shRUNX2* generated an ~80% decrease in *VIMENTIN* expression. In breast cancer cells, it has been reported that RUNX2 increases *VIMENTIN* and *SNAIL2* expression.[39,40] Likewise, *VIMENTIN* is an osteogenic differentiation master TF target gene, as is RUNX2[29,30,41] In conclusion, *RUNX2* overexpression in lung cancer was related with EMT process, through direct regulation of *E-CADHERIN, VIMENTIN, TWIST1,* and *SNAIL1* expression.[29,30] Therefore, it could become a new therapeutic target for patients with NSCLC.

Declaration of conflicting interests

The author(s) declared no potential conflicts of interest with respect to the research, authorship, and/or publication of this article.

Funding

ORCID iDs

Andrea Carolina Ramírez https://orcid.org/0000-0002-4785-6848
Adriana P Rojas https://orcid.org/0000-0001-8528-4433

Supplemental material

Supplemental material for this article is available online.

References

1. Torre LA, Bray F, Siegel RL, et al. Global cancer statistics, 2012. *CA Cancer J Clin* 2015; 65: 87–108.
2. Siegel RL, Miller KD and Jemal A. Cancer statistics, 2015. *CA Cancer J Clin* 2015; 65: 5–29.
3. Feachem RG, Graham WJ and Timaeus IM. Identifying health problems and health research priorities in developing countries. *J Trop Med Hyg* 1989; 92(3): 133–191.
4. Hossfeld DK. World Health Organization classification of tumours: pathology and genetics of tumours of haematopoietic and lymphoid tissues. In: Jaffe ES, Harris NL, Stein H, et al. (eds) *Annals of oncology*, vol. 13. Lyon: IARC Press, 2002, pp. 490–491.
5. Harb OA, El Shorbagy S, Abouhashem NS, et al. Cripto-1 and RUNX2 expressions in non-small cell lung cancer, their roles in its progression and patients outcome. *J Clin Expert Oncol* 2017; 6: 1–12.
6. Hanahan D and Weinberg RA. Hallmarks of cancer: the next generation. *Cell* 2011; 144: 646–674.
7. Marcucci F, Stassi G and De Maria R. Epithelial-mesenchymal transition: a new target in anticancer drug discovery. *Nat Rev Drug Discov* 2016; 15(5): 311–325.
8. Zha L, Cao Q, Cui X, et al. Epigenetic regulation of E-cadherin expression by the histone demethylase UTX in colon cancer cells. *Med Oncol* 2016; 33(3): 21.
9. Troncoso D, Perpiñan IM, Mancera SAA, et al. Transición epitelio mesénquima: de lo molecular a lo fisiológico. *Univ Médica* 2017; 58: 1–10.
10. Heerboth S, Housman G, Leary M, et al. EMT and tumor metastasis. *Clin Transl Med* 2015; 4: 6.
11. Vesuna F, Van Diest P, Chen JH, et al. Twist is a transcriptional repressor of E-cadherin gene expression in breast cancer. *Biochem Biophys Res Commun* 2008; 367(2): 235–241.
12. Zhuo W-L, Wang Y, Zhuo X-L, et al. Short interfering RNA directed against TWIST, a novel zinc finger transcription factor, increases A549 cell sensitivity to cisplatin via MAPK/mitochondrial pathway. *Biochem Biophys Res Commun* 2008; 369(4): 1098–1102.
13. Roberts CM, Tran MA, Pitruzzello MC, et al. TWIST1 drives cisplatin resistance and cell survival in an ovarian cancer model, via upregulation of GAS6, L1CAM, and Akt signalling. *Sci Rep* 2016; 6: 37652.
14. Miyoshi A, Kitajima Y, Kido S, et al. Snail accelerates cancer invasion by upregulating MMP expression and is associated with poor prognosis of hepatocellular carcinoma. *Br J Cancer* 2005; 92(2): 252–258.
15. Ho WP, Chan WP, Hsieh MS, et al. Runx2-mediated bcl-2 gene expression contributes to nitric oxide protection against hydrogen peroxide-induced osteoblast apoptosis. *J Cell Biochem* 2009; 108(5): 1084–1093.
16. Ito Y, Bae S-C and Chuang LSH. The RUNX family: developmental regulators in cancer. *Nat Rev Cancer* 2015; 15(2): 81–95.
17. Sancisi V, Manzotti G, Gugnoni M, et al. RUNX2 expression in thyroid and breast cancer requires the cooperation of three non-redundant enhancers under the control of BRD4 and c-JUN. *Nucleic Acids Res* 2017; 45(19): 11249–11267.
18. Li YL and Xiao ZS. Advances in Runx2 regulation and its isoforms. *Med Hypotheses* 2007; 68(1): 169–175.
19. Pratap J, Lian JB, Javed A, et al. Regulatory roles of Runx2 in metastatic tumor and cancer cell interactions with bone. *Cancer Metastasis Rev* 2006; 25(4): 589–600.
20. Li H, Zhou R-J, Zhang G-Q, et al. Clinical significance of RUNX2 expression in patients with nonsmall cell lung cancer: a 5-year follow-up study. *Tumour Biol* 2013; 34(3): 1807–1812.
21. Niu DF, Kondo T, Nakazawa T, et al. Transcription factor Runx2 is a regulator of epithelial-mesenchymal transition and invasion in thyroid carcinomas. *Lab Invest* 2012; 92(8): 1181–1190.
22. Yuen H-F, Kwok W-K, Chan K-K, et al. TWIST modulates prostate cancer cell-mediated bone cell activity and is upregulated by osteogenic induction. *Carcinogenesis* 2008; 29(8): 1509–1518.
23. Tandon M, Gokul K, Ali SA, et al. Runx2 mediates epigenetic silencing of the bone morphogenetic protein-3B (BMP-3B/GDF10) in lung cancer cells. *Mol Cancer* 2012; 11: 27.

24. Herreño AM, Fernández MJ, Rey L, et al. Primary lung cancer cell culture from transthoracic needle biopsy samples. *Cogent Med* 2018; 5: 1503071.

25. Zhang X, Li Y, Zhang Y, et al. Beta-elemene blocks epithelial-mesenchymal transition in human breast cancer cell line MCF-7 through Smad3-mediated down-regulation of nuclear transcription factors. *PLoS ONE* 2013; 8(3): e58719.

26. Abramoff MD, Magelhaes PJ and Ram SJ. Image processing with ImageJ. *J Biophotonics* 2004; 11: 36–42.

27. Rojas A, Aguilar R, Henriquez B, et al. Epigenetic control of the bone-master Runx2 gene during osteoblast-lineage commitment by the histone demethylase JARID1B/KDM5B. *J Biol Chem* 2015; 290(47): 28329–28342.

28. Rojas A, Sepulveda H, Henriquez B, et al. Mll-COMPASS complexes mediate H3K4me3 enrichment and transcription of the osteoblast master gene Runx2/p57 in osteoblasts. *J Cell Physiol* 2019; 234: 6244–6253.

29. Bradner JE, Hnisz D and Young RA. Transcriptional addiction in cancer. *Cell* 2017; 168: 629–643.

30. Sancisi V, Gandoli G, Ambrosetti DC, et al. Histone deacetylase inhibitors repress tumoral expression of the proinvasive factor Runx2. *Cancer Res* 2015; 75: 1868–1882.

31. Maier T, Güell M and Serrano L. Correlation of mRNA and protein in complex biological samples. *FEBS Lett* 2009; 583(24): 3966–3973.

32. Rami-Porta R, Asamura H, Brierley J, et al. Staging, tumor profile, and prognostic groups in lung cancer or the new tower of Babel. *J Thorac Oncol* 2016; 11(8): 1201–1203.

33. Sze CC and Shilatifard A. MLL3/MLL4/COMPASS family on epigenetic regulation of enhancer function and cancer. *Cold Spring Harb Perspect Med* 2016; 6: a026427.

34. Voon DC and Thiery JP. The emerging roles of RUNX transcription factors in epithelial-mesenchymal transition. *Adv Exp Med Biol* 2017; 962: 471–489.

35. Adhikary A, Chakraborty S, Mazumdar M, et al. Inhibition of epithelial to mesenchymal transition by E-cadherin up-regulation via repression of slug transcription and inhibition of E-cadherin degradation: dual role of scaffold/matrix attachment region-binding protein 1 (SMAR1) in breast cancer cells. *J Biol Chem* 2014; 289(37): 25431–25444.

36. Li Q, Zhao H, Xia S, et al. RUNX2 promotes epithelial differentiation of ADSCs and burn wound healing via targeting E-cadherin. *Oncotarget* 2017; 9: 2646–2659.

37. Hsu YL, Huang MS, Yang CJ, et al. Lung tumor-associated osteoblast-derived bone morphogenetic protein-2 increased epithelial-to-mesenchymal transition of cancer by Runx2/Snail signaling pathway. *J Biol Chem* 2011; 286(43): 37335–37346.

38. Puisieux A, Valsesia-Wittmann S and Ansieau S. A twist for survival and cancer progression. *Br J Cancer* 2006; 94(1): 13–17.

39. Hon GC, Hawkins RD, Caballero OL, et al. Global DNA hypomethylation coupled to repressive chromatin domain formation and gene silencing in breast cancer. *Genome Res* 2012; 22(2): 246–258.

40. Chimge NO, Baniwal SK, Little GH, et al. Regulation of breast cancer metastasis by Runx2 and estrogen signaling: the role of SNAI2. *Breast Cancer Res* 2011; 13(6): R127.

41. Lian N, Wang W, Li L, et al. Vimentin inhibits ATF4-mediated osteocalcin transcription and osteoblast differentiation. *J Biol Chem* 2009; 284(44): 30518–30525.